

# Resource-efficient analyzer of Bell and Greenberger-Horne-Zeilinger states of multiphoton systems

Tao Li<sup>1,2</sup>, Adam Miranowicz<sup>2,3</sup>, Keyu Xia<sup>4</sup>, and Franco Nori<sup>2,5</sup>

<sup>1</sup>*School of Science, Nanjing University of Science and Technology, Nanjing 210094, China*

<sup>2</sup>*Theoretical Quantum Physics Laboratory, RIKEN Cluster for Pioneering Research, Wako-shi, Saitama 351-0198, Japan*

<sup>3</sup>*Faculty of Physics, Adam Mickiewicz University, 61-614 Poznań, Poland*

<sup>4</sup>*College of Engineering and Applied Sciences, Nanjing University, Nanjing 210093, China*

<sup>5</sup>*Physics Department, The University of Michigan, Ann Arbor, Michigan 48109-1040, USA*

(Dated: June 13, 2022)

We propose a resource-efficient error-rejecting entangled-state analyzer for polarization-encoded multiphoton systems. The analyzer works in a passive way and can completely distinguish  $2^n$  Greenberger-Horne-Zeilinger (GHZ) states of  $n$  photons without using any active operation or fast switching. The efficiency and fidelity of the GHZ-state analysis can, in principle, be close to unity, when an ideal single-photon scattering condition is fulfilled. For a non-ideal scattering, which typically reduces the fidelity of a GHZ-state analysis, we introduce a passively error-rejecting circuit to enable a near-perfect fidelity at the expense of a slight decrease of its efficiency. Furthermore, the protocol can be directly used to perform a two-photon Bell-state analysis. This passive, resource-efficient, and error-rejecting protocol can, therefore, be useful for practical quantum networks.

## I. INTRODUCTION

Quantum entanglement is a fascinating phenomena in quantum physics [1], which provides a promising platform for various quantum technologies, including quantum communication networks [2]. Sharing quantum entanglement among distant network nodes is a prerequisite for, e.g., distributed quantum computation [3–6], quantum key distribution [7], quantum teleportation [8], and quantum secure direct communication [9–12], among others. There are two main obstacles for practical applications of multipartite quantum entanglement, i.e., entanglement generation over desired nodes and entanglement analysis within a local node. Usually, it is difficult to distribute a local entanglement over spatially-separated nodes, since, e.g., the channel noise introduces an exponential decay of an entangled photon pair when its photons are distributed to two quantum network nodes [13]. An efficient method to overcome the channel decoherence can be based on quantum repeaters [14–17], which are based on entanglement-purification protocols [18–21] and quantum swapping [22–26]. By applying a proper entanglement analysis and local operations, one can complete an entanglement-purification protocol to distill some entanglement of a higher fidelity, and enlarge the distance of an entangled channel through quantum swapping. For these and other reasons, the analysis of entanglement plays an essential role in various entanglement-based quantum information processing protocols [7–26].

Multipartite entanglement [27–29] compared to two-particle entanglement, can be used to build more complex quantum networks involving many nodes [30–33] and to constitute a building block for measurement-based quantum computing [34–40]. The Greenberger-Horne-Zeilinger (GHZ) states are among the most important kinds of multipartite entanglement [27–29]. The generation and analysis of the GHZ entanglement are highly demanded. To date, various efficient methods

to generate the GHZ entanglement have been developed for a diversity of physical systems [41–48]. In photonic systems, an eight-photon GHZ state and a three-photon high-dimensional GHZ state have been experimentally demonstrated [49–52] by performing quantum fusion combined with post-selection operations and quantum interference [27, 53, 54]. By using a time delay, a resource-efficient method was proposed and experimentally demonstrated for generating a six-photon GHZ state with only one spontaneous parametric down-conversion source [55]. It is possible to generate photonic GHZ states or other multipartite entanglement in a deterministic way [56–60], assisted by nonlinear processes such as the cross-Kerr nonlinearity or the nonlinearity induced by the light-atom interaction in an optical cavity. However, it is difficult to distribute such a GHZ state efficiently to distant nodes, due to the inefficiency of the GHZ sources and high losses during transmission [13, 61]. One possible solution is to establish entanglement pairs between a center node and distant nodes in parallel [14–17], and then to perform a quantum swapping together with a GHZ-state analysis in the center node [62, 63]. In this way, multipartite entanglement among distant nodes can be generated and distributed for complex quantum networks.

A partial entanglement analysis for GHZ states can be performed with similar processes as those used for the GHZ-state generation. In 1998, Pan and Zeilinger proposed, to our knowledge, the first practical GHZ-state analysis with linear-optical elements [64]. Their proposal can identify two of  $n$ -photon GHZ states by post-selection operations. In principle, one can constitute a nearly deterministic  $n$ -photon GHZ-state analysis with linear optics, when massive ancillary photons are used [65]. However, according to the Cansamiglia-Lütkenhaus no-go theorem [66]: Perfect and deterministic Bell-state analysis on two polarization-encoded qubits is impossible by using only linear-optical elements (in

addition to photodetectors) and auxiliary modes in the vacuum state. More specifically, “it is not possible to discriminate unambiguously four equiprobable Bell states with a probability higher than 50%” by using solely these resources. By taking into account nonlinear processes, a complete GHZ-state analysis for photonic systems becomes possible [67, 68], and can achieve perfect efficiency and fidelity for an ideal process. Moreover, an entangled-state analysis has been proposed for redundantly or hyperentangled encoded photon pairs recently [69–74]. The existing GHZ-state analyzers typically require active operations and/or fast switching, and, therefore, always require more quantum resources when the photon number of a given GHZ state increases. Furthermore, the fidelity of a Bell-state or GHZ-state analyses significantly depend on the nonlinearity strength of realistic nonlinear processes [60]. A deviation from an ideal nonlinear process leads to errors and, thus, reduces the fidelity. These aforementioned disadvantages significantly limit applications of a GHZ-state analysis for practical quantum networks.

Here we propose a resource-efficient passive protocol of a multiphoton GHZ-state analysis using only two single-photon nondestructive (quantum nondemolition, QND) detectors and standard (destructive) single-photon detectors, and some linear-optical elements. The GHZ-state analysis circuit is universal, and can completely distinguish GHZ states with different photon numbers, according to the measurement results of our single-photon nondestructive and destructive detectors. During the entangled-state analysis, there are neither active operations on ancillary atoms nor adaptive switching of photons [75]. The circuit works in a passive way as the Pan-Zeilinger GHZ analyzer does [64]. The efficiency of our GHZ-state analysis can, in principle, be equal to one and can completely distinguish  $2^n$  GHZ states of an  $n$ -photon system and two-photon Bell states. Moreover, our protocol has no requisite for direct Hong-Ou-Mandel interference which requires simultaneous operations on two individual photons. Thus, we can significantly simplify the process of GHZ-state analysis and, subsequently, the structure of multinode quantum networks. Furthermore, the detrimental effect on the fidelity, introduced by a non-ideal scattering process, can be eliminated passively at the expense of a decrease of its efficiency. Therefore, our protocol is resource-efficient and passive, and can be used to efficiently entangle distant nodes in complex quantum networks.

The paper is organized as follows: A quantum interface between a single photon and a single quantum dot (QD) is introduced briefly in Sec. II for performing QND measurements on linearly-polarized photons. In Sec. III, a passive GHZ-state analysis circuit is presented composed of simple linear-optical elements, as well as single-photon nondestructive and destructive detectors. In Sec. IV, a method to efficiently generate entanglement among distant nodes is presented with this GHZ-state analysis circuit. Subsequently, the performance of the circuit with

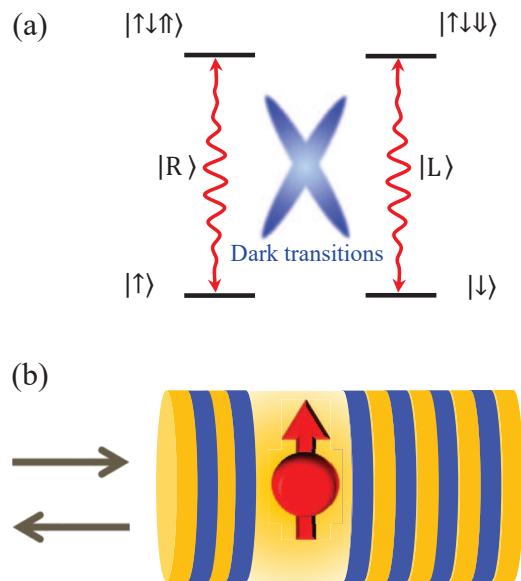


FIG. 1: Spin-dependent transitions for the negatively-charged exciton  $X^-$ . (a) Relative-level structure and optical transition of a singly-charged quantum dot (QD), (b) a QD coupled to an optical micropillar cavity. Here,  $|\uparrow\rangle$  ( $|\downarrow\rangle$ ) denotes the electron spin state with  $J_z$  equal to  $1/2$  ( $-1/2$ ), and  $|\uparrow\downarrow\uparrow\rangle$  ( $|\uparrow\downarrow\downarrow\rangle$ ) denotes the trion state of  $X^-$  with  $J_z$  equal to  $3/2$  ( $-3/2$ ). A photon in a right- (left-) circularly-polarized state  $|R\rangle$  ( $|L\rangle$ ) can only couple to the transition  $|\uparrow\rangle \leftrightarrow |\uparrow\downarrow\uparrow\rangle$  ( $|\downarrow\rangle \leftrightarrow |\uparrow\downarrow\downarrow\rangle$ ). Therefore, the cross transitions are forbidden by the quantum-optical selection rules.

state-of-the-art experimental parameters is discussed in Sec. V. Finally, we conclude with a brief discussion and summary in Sec. VI.

## II. SINGLE-PHOTON QND DETECTOR

An efficient interface, between a single photon and a single emitter, constitutes a necessary building block for various kinds of quantum tasks, especially for long-distance or distributed quantum networks [2, 60]. To begin with, we consider a process of single-photon scattering by a four-level emitter coupled to a one-dimensional system, such as a QD coupled to a micropillar cavity or a photonic nanocrystal waveguide [76–81]. A singly-charged self-assembled In(Ga)As QD has four energy levels [80–82]: two ground states of  $J_z = \pm 1/2$ , denoted as  $|\uparrow\rangle$  and  $|\downarrow\rangle$ , respectively; and two optically-excited trion states  $X^-$ , consisting of two electrons and one hole, with  $J_z = \pm 3/2$ , denoted as  $|\uparrow\downarrow\uparrow\rangle$  and  $|\uparrow\downarrow\downarrow\rangle$ , respectively. Here the quantization axis  $z$  is along the growth direction of the QD and it is the same as the direction of the input photon. Therefore, there are two circularly-polarized dipole transmissions which are degenerated when the environment magnetic field is zero, as shown in Fig. 1. A right-circularly polarized photon  $|R\rangle$  and a left-circularly

polarized photon  $|L\rangle$  can only couple to the transitions  $|\uparrow\rangle \leftrightarrow |\uparrow\downarrow\uparrow\rangle$  and  $|\downarrow\rangle \leftrightarrow |\uparrow\downarrow\downarrow\rangle$ , respectively.

The single-photon scattering process of a QD-cavity unit is dependent on the state of the QD. There are two individual cases: (1) If an input photon does not match the circularly-polarized transition of the QD, the photon excites the cavity mode that is orthogonal to the polarization transition of the QD, and it is reflected by a practically empty cavity with a loss probability caused by photon absorption and/or side leakage. (Hereafter, for brevity, we refer to the side leakage only, but we also mean other photon absorption losses.) However, (2) if an input photon matches a given transition of the QD, the photon interacts with the QD and is reflected by the cavity that couples to the QD. Therefore, a  $j$ -circularly polarized photon (where  $j = \text{right or left}$ ) in the input mode  $\hat{a}_{\omega_j, \text{in}}^\dagger$  of frequency  $\omega_j$ , after it is scattered by a QD-cavity unit, evolves into an output mode  $\hat{a}_{\omega_j, \text{out}}^\dagger$  as follows [79–82]:

$$\begin{aligned} \hat{a}_{\omega_j, \text{in}}^\dagger |0, 0, \bar{s}\rangle &\rightarrow r_0 \hat{a}_{\omega_j, \text{out}}^\dagger |0, 0, \bar{s}\rangle, \\ \hat{a}_{\omega_j, \text{in}}^\dagger |0, 0, s\rangle &\rightarrow r_1 \hat{a}_{\omega_j, \text{out}}^\dagger |0, 0, s\rangle, \end{aligned} \quad (1)$$

where the state  $|0, 0, s\rangle$  ( $|0, 0, \bar{s}\rangle$ ) denotes that both input and output fields are in the vacuum state and the QD is in the state  $|s\rangle$  ( $|\bar{s}\rangle$ ) that couples (does not couple) to the input photon. The state-dependent reflection amplitudes  $r_0$  and  $r_1$ , corresponding, respectively, to the aforementioned cases (1) and (2), are given by [79–82]:

$$\begin{aligned} r_0(\omega) &= 1 - \frac{\kappa}{i(\omega_c - \omega) + \frac{\kappa}{2} + \frac{\kappa_s}{2}}, \\ r_1(\omega) &= 1 - \frac{\kappa f}{[i(\omega_c - \omega) + \frac{\kappa}{2} + \frac{\kappa_s}{2}]f + g^2}, \end{aligned} \quad (2)$$

where the auxiliary function  $f$  is given by  $f = i(\omega_{X-} - \omega) + \frac{\gamma}{2}$ . Here  $\omega_{X-}$  is the transmission frequency of the QD and  $\omega_c$  is the resonant frequency of the cavity. These frequencies can be tuned to be equal with  $\omega_{X-} = \omega_c$ , for simplicity. Moreover,  $\kappa$  describes a directional coupling between the cavity modes and the input and output modes;  $g$  denotes the coupling between the QD and cavity;  $\kappa_s$  represents the cavity side leakage rate, and  $\gamma$  is the trion decay rate.

For ideal scattering with  $\kappa_s \ll \kappa$  and  $\gamma, \kappa \ll g$ , an input photon, that is resonant with a QD transition, is deterministically reflected by the QD-cavity unit. A  $\pi$ -phase (*zero*-phase) shift is introduced to the hybrid system consisting of a photon and the QD with  $r_0 = -1$  ( $r_1 = 1$ ), if the photon decouples (couples) to a transition of the QD. When the QD is initialized to be in the superposition state  $|\pm\rangle = (|\uparrow\rangle \pm |\downarrow\rangle)/\sqrt{2}$ , an input photon in a linearly-polarized state evolves as follows:

$$\begin{aligned} |H\rangle|\pm\rangle &\rightarrow |V\rangle|\mp\rangle, \\ |V\rangle|\pm\rangle &\rightarrow |H\rangle|\mp\rangle, \end{aligned} \quad (3)$$

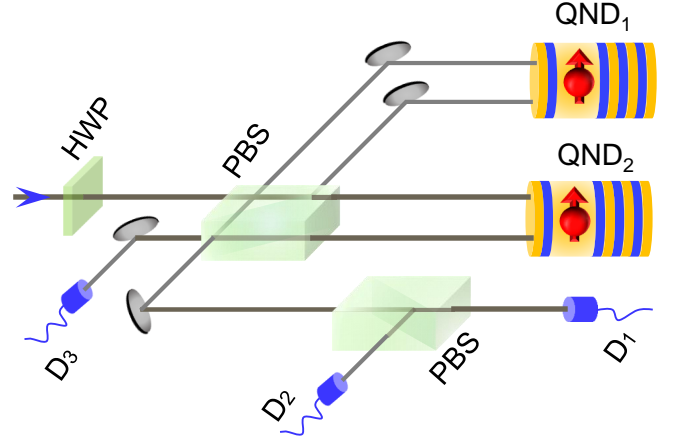


FIG. 2: Schematics of the passive optical GHZ-state analyzer using single-photon QND detectors. Here PBS denotes a polarizing beam splitter, which transmits photons with horizontal polarization  $|H\rangle$  and reflects those with vertical polarization  $|V\rangle$ . HWP represents a half-wave plate that performs the Hadamard transformation on photons passing it, i.e.,  $|H\rangle \rightarrow (|H\rangle + |V\rangle)/\sqrt{2}$  or  $|V\rangle \rightarrow (|H\rangle - |V\rangle)/\sqrt{2}$ . QND detection completes a nondestructive measurement on single photons, and  $D_i$  ( $i = 1, 2, 3$ ) is an ordinary (destructive) single-photon detector.

which means that the QD can be used as a QND detector for linearly-polarized photons [80, 83, 84]. This is because the QD state is flipped to an orthogonal state after a linearly-polarized photon is reflected by the QD-cavity unit [85, 86]. Simultaneously, the polarization state of the photon is also flipped, which can significantly simplify the passive GHZ-state analysis under practical scattering conditions.

### III. PASSIVE GHZ-STATE ANALYZER

So far, we have described a QND detection of linearly-polarized single photons. In the following section, we describe how to incorporate the QND into the setup for the passive optical GHZ-state analysis, as shown in Fig. 2. The setup is composed of a half-wave plate (HWP), two polarizing beam splitters (PBSs), two single-photon QND detectors, and several standard (destructive) single-photon detectors. The HWP is tuned to perform the Hadamard transformation on photons passing it, i.e.,  $|H\rangle \rightarrow (|H\rangle + |V\rangle)/\sqrt{2}$  or  $|V\rangle \rightarrow (|H\rangle - |V\rangle)/\sqrt{2}$ . The PBS transmits linearly-polarized photons in the state  $|H\rangle$  and reflects photons in the state  $|V\rangle$ . The single-photon QND and standard detectors complete the photon on-off measurements in nondestructive and destructive ways, respectively.

For  $n$ -photon polarization-encoded GHZ states, the

simplest two can be expressed as [27]

$$\begin{aligned} |\text{GHZ}_{00\dots 0}^+\rangle &= \frac{1}{\sqrt{2}} (|H\rangle^{\otimes n} + |V\rangle^{\otimes n}), \\ |\text{GHZ}_{00\dots 0}^-\rangle &= \frac{1}{\sqrt{2}} (|H\rangle^{\otimes n} - |V\rangle^{\otimes n}), \end{aligned} \quad (4)$$

which means that if a photon is determined in a state  $|H\rangle$  or  $|V\rangle$ , the remaining  $(n-1)$  photons are collapsed into the same polarization state. To constitute a complete basis for the  $n$ -photon system, one should take the remaining  $2^{n-1}$  orthogonal basis states into consideration,

$$\begin{aligned} |\text{GHZ}_{i_1 i_2 \dots i_n}^+\rangle &= \bigotimes_{j=1}^n \sigma_{x_j}^{i_j} |\text{GHZ}_{00\dots 0}^+\rangle, \\ |\text{GHZ}_{i_1 i_2 \dots i_n}^-\rangle &= \bigotimes_{j=1}^n \sigma_{x_j}^{i_j} |\text{GHZ}_{00\dots 0}^-\rangle, \end{aligned} \quad (5)$$

which can be generated from  $|\text{GHZ}_{00\dots 0}^\pm\rangle$  by performing a single-photon rotation on each photon with  $\bigotimes_{j=1}^n \sigma_{x_j}^{i_j} = \sigma_{x_1}^{i_1} \otimes \sigma_{x_2}^{i_2} \otimes \dots \otimes \sigma_{x_n}^{i_n}$ . Here superscripts  $i_1, i_2, \dots$ , and  $i_n \in \{0, 1\}$  with  $\sum_j i_j \leq n/2$ , the Pauli operators  $\sigma_{x_j} = |H\rangle\langle V| + |V\rangle\langle H|$  perform a polarization flip on the  $j$ th photon with  $j = 1, 2, \dots$ , and  $n$ . Therefore, any  $n$ -photon pure state can be represented by a superposition state of these  $2^n$  GHZ states.

Now we focus on completely distinguishing the aforementioned  $2^n$  GHZ states, which is of vital importance for multiuser quantum networks [62–64]. For clarity, we divide this state analysis into several steps. Let us suppose that there is a spatial separation between optical elements such that all photons can pass a given optical element before entering another element. Note this requirement is not necessary, and we will demonstrate, in the next section, that our proposal also works when each photon is passing one by one from the input port to the output port, when it is measured by a single-photon destructive detectors.

After passing  $n$  photons through the HWP, the Hadamard transformation is performed on each photon, and the  $2^n$  GHZ states are changed into superposition states of  $2^{n-1}$  states. For instance, the states  $|\text{GHZ}_{00\dots 0}^+\rangle$  and  $|\text{GHZ}_{00\dots 0}^-\rangle$ , after the Hadamard transformation of each photon, evolve into

$$\begin{aligned} |\text{GHZ}_{00\dots 0}^+\rangle_1 &= \sum_{l=0}^{n'} \left[ \bigotimes_{j=1}^n \sigma_{x_j}^{i_j} |H\rangle^{\otimes n} \right], \\ |\text{GHZ}_{00\dots 0}^-\rangle_1 &= \sum_{m=1}^{n'} \left[ \bigotimes_{k=1}^n \sigma_{x_k}^{i_k} |H\rangle^{\otimes n} \right], \end{aligned} \quad (6)$$

respectively. Here  $\sum_j i_j = 2l$  for  $l \leq n/2$ , and  $\sum_k i_k = 2m+1$  for  $m \leq n/2$ . That is, the state  $|\text{GHZ}_{00\dots 0}^+\rangle_1$  ( $|\text{GHZ}_{00\dots 0}^-\rangle_1$ ) is constituted by the states of all even (odd) numbers of  $|V\rangle$  polarized photons, and the relative phase between each two components is *zero*.

The photons, after passing through the HWP, are either transmitted or reflected by the first PBS, which is followed by a QD-cavity unit (referred to as a QND detector) in each output modes. As demonstrated in Sec. II, a linearly-polarized photon, after being scattered by a QND detector, flips the state of the detector QD and the state polarization is changed into an orthogonal state. There are two cases:

(i) If the  $n$  photons are in the state  $|\text{GHZ}_{00\dots 0}^+\rangle_1$ , they flip the state of either QD once when each photon is scattered by the corresponding QND detector. Finally, the QD in QND<sub>1</sub> is projected into the state  $|+\rangle$ , while the QD in QND<sub>2</sub> is projected into the state  $|+\rangle$  ( $|-\rangle$ ) for an even (odd)  $n$ .

(ii) However, if the  $n$  photons are in the state  $|\text{GHZ}_{00\dots 0}^-\rangle_1$ , they flip the states of the QDs as well, and project the QD in QND<sub>1</sub> into the state  $|-\rangle$  and project the QD in QND<sub>2</sub> into the state  $|-\rangle$  ( $|+\rangle$ ) when  $n$  is even (odd).

When all the photons are scattered by the QND detectors, the hybrid state of the two QDs and the  $n$  photons evolves into

$$\begin{aligned} |\text{GHZ}_{00\dots 0}^+\rangle_2 &= \sum_{l=0}^{n'} \left[ \bigotimes_{j=1}^n \sigma_{x_j}^{i_j+1} |H\rangle^{\otimes n} |+\rangle_1 |+\rangle_2 \right], \\ |\text{GHZ}_{00\dots 0}^-\rangle_2 &= \sum_{m=1}^{n'} \left[ \bigotimes_{k=1}^n \sigma_{x_k}^{i_k+1} |H\rangle^{\otimes n} |-\rangle_1 |-\rangle_2 \right], \end{aligned} \quad (7)$$

if  $n$  is even, and into

$$\begin{aligned} |\text{GHZ}_{00\dots 0}^+\rangle_2 &= \sum_{l=0}^{n'} \left[ \bigotimes_{j=1}^n \sigma_{x_j}^{i_j+1} |H\rangle^{\otimes n} |+\rangle_1 |-\rangle_2 \right], \\ |\text{GHZ}_{00\dots 0}^-\rangle_2 &= \sum_{m=1}^{n'} \left[ \bigotimes_{k=1}^n \sigma_{x_k}^{i_k+1} |H\rangle^{\otimes n} |-\rangle_1 |+\rangle_2 \right], \end{aligned} \quad (8)$$

if  $n$  is odd. We can deterministically distinguish  $|\text{GHZ}_{00\dots 0}^+\rangle_1$  and  $|\text{GHZ}_{00\dots 0}^-\rangle_1$  for both cases of even and odd  $n$ , according to the state of the QDs in QND detectors.

To make this point clearer, we continue our analysis with an arbitrary *even*  $n$  only. Now, photons in different polarization states combine again at the first PBS, which is followed by a HWP. The HWP completes the Hadamard transformation on each photon passing through it. Thus, the hybrid state, as given in Eq. (7), evolves into

$$\begin{aligned} |\text{GHZ}_{00\dots 0}^+\rangle_3 &= |\text{GHZ}_{00\dots 0}^-\rangle |+\rangle_1 |+\rangle_2, \\ |\text{GHZ}_{00\dots 0}^-\rangle_3 &= |\text{GHZ}_{00\dots 0}^+\rangle |-\rangle_1 |-\rangle_2. \end{aligned} \quad (9)$$

Here  $|\text{GHZ}_{00\dots 0}^+\rangle$  and  $|\text{GHZ}_{00\dots 0}^-\rangle$  are two  $n$ -photon GHZ states given in Eq. (4). Subsequently, a photon-polarization measurement setup, consisting of a PBS and two destructive single-photon detectors D<sub>1</sub> and D<sub>2</sub>, is used to detect the polarization of each photon and then



	$ HH\rangle/ VV\rangle$	$ HV\rangle/ VH\rangle$	$ ++\rangle$	$ --\rangle$
$ \phi^+\rangle$	✓		✓	
$ \phi^-\rangle$	✓			✓
$ \psi^+\rangle$		✓		✓
$ \psi^-\rangle$		✓	✓	

TABLE I: Complete two-photon Bell-state analysis. Here  $|ij\rangle$  represents the measurement result of the two single-photon detectors (QDs) with  $|ij\rangle = \{|HH\rangle, |VV\rangle, |HV\rangle, |VH\rangle\}$  ( $|ij\rangle = \{|++\rangle, |--\rangle\}$ ). We use the standard notation for the Bell states  $|\phi^\pm\rangle$  and  $|\psi^\pm\rangle$ , as given in Eq. (10).

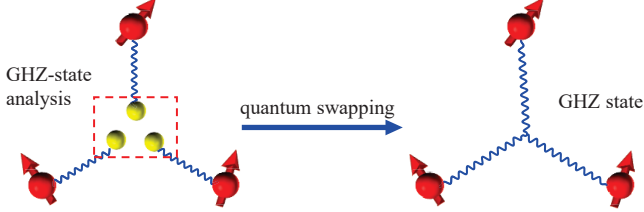


FIG. 3: Schematics of nonlocal GHZ-state generation for multiparty quantum networks. Here a red circle with an arrow represents a stationary qubit, while a yellow circle represents a photon. Each wave line represents entanglement between the particles it connects.

divide the measurement results according to the number of clicks of each detector. Finally, a measurement of the QD in each QND detector is performed, which finishes the passive polarization-encoded GHZ states analysis.

So far, we have described the evolution of two particular polarization-encoded  $n$ -photon GHZ states  $|\text{GHZ}_{00\dots0}^+\rangle$  and  $|\text{GHZ}_{00\dots0}^-\rangle$ . That is, when  $n$   $H$ -polarized ( $V$ -polarized) photons are detected, the  $n$  input photons are projected into either  $|\text{GHZ}_{00\dots0}^+\rangle$  or  $|\text{GHZ}_{00\dots0}^-\rangle$ , which can be subsequently distinguished by detecting the state of the QD in each QND detector, as given in Eqs. (7) and (8). Using a similar entanglement analysis, we can also completely distinguish  $2^n$  GHZ states for  $n$  polarization-encoded photons. When  $n = 2$ , the GHZ-state analysis setup enables a passive Bell-state analysis for two-photon systems, which are typically denoted as

$$\begin{aligned} |\phi^\pm\rangle &= \frac{1}{\sqrt{2}} (|H\rangle|H\rangle \pm |V\rangle|V\rangle), \\ |\psi^\pm\rangle &= \frac{1}{\sqrt{2}} (|H\rangle|V\rangle \pm |V\rangle|H\rangle). \end{aligned} \quad (10)$$

It is seen that there is neither active feedback nor fast switching operations involved in the entangled-state analysis. The setup works in a completely passive way, which is similar to that based on linear-optical elements and single-photon detectors. The results for two specific cases with  $n = 2$  and  $n = 3$  are given in Tables I and II, respectively.

	C1	C2	C3	C4	$  - + \rangle$	$  + - \rangle$
$ \text{GHZ}_{000}^+\rangle$	✓				✓	
$ \text{GHZ}_{000}^-\rangle$	✓					✓
$ \text{GHZ}_{100}^+\rangle$		✓			✓	
$ \text{GHZ}_{100}^-\rangle$		✓				✓
$ \text{GHZ}_{010}^+\rangle$			✓		✓	
$ \text{GHZ}_{010}^-\rangle$			✓			✓
$ \text{GHZ}_{001}^+\rangle$				✓	✓	
$ \text{GHZ}_{001}^-\rangle$				✓		✓

TABLE II: Complete three-photon GHZ-state analysis. Here the measurement results C1, C2, C3, and C4 of the two single-photon detectors D<sub>1</sub> and D<sub>2</sub> correspond to  $|HHH\rangle/|VVV\rangle$ ,  $|HVV\rangle/|VHH\rangle$ ,  $|VHV\rangle/|HVH\rangle$ , and  $|VVH\rangle/|HHV\rangle$ , respectively.  $| - + \rangle$  and  $| + - \rangle$  denotes two possible results of the measurement on the two QDs.

#### IV. EFFICIENT DISTANT MULTIPARTITE ENTANGLEMENT GENERATION FOR QUANTUM NETWORKS

In quantum multinode networks, multipartite entanglement among many nodes is useful for practical quantum communication or distributed quantum computation [27, 28]. A direct method for sharing the GHZ entanglement among several distant nodes can be enabled by a faithful entanglement distribution after locally generating the GHZ entanglement. However, the efficiency of such a multipartite entanglement distribution significantly decreases with the increasing photon number involved in the GHZ entanglement [13]. Furthermore, the experimental methods for generating multiphoton GHZ entanglement are still inefficient due to the limited experimental technologies. A significantly more efficient method for distant GHZ entanglement generation can be achieved by entanglement swapping. In the following, we describe a scheme for the GHZ entanglement generation among three stationary qubits, and these stationary qubits can be atomic ensembles, nitrogen-vacancy (NV) centers, QDs, and other systems [87].

Suppose there are three communicating nodes in a quantum network, say, Alice, Bob, and Charlie. An ancillary node (Eve) shares hybrid entanglement pairs with Alice, Bob, and Charlie, respectively, as follows [14–21]:

$$|\phi\rangle_{ji} = \frac{1}{\sqrt{2}} (|H\rangle_i |\uparrow\rangle_j + |V\rangle_i |\downarrow\rangle_j), \quad (11)$$

where the subscript  $i$  (with  $i = a, b, c$ ) represents the photons owned by Eve, and it is entangled with the  $j$ th QD (with  $j = A, B, C$ ), which belongs to Alice, Bob, and Charlie, respectively. The state  $|\phi\rangle_{Aa}|\phi\rangle_{Bb}|\phi\rangle_{Cc}$  of the three hybrid entanglement pairs  $Aa$ ,  $Bb$ , and  $Cc$  can

be rewritten as

$$|\Phi\rangle_0 = \sum_{i,j,k} \frac{1}{2\sqrt{2}} \left( |\text{GHZ}_{ijk}^+\rangle_{ABC} |\text{GHZ}_{ijk}^+\rangle_{abc} + |\text{GHZ}_{ijk}^-\rangle_{ABC} |\text{GHZ}_{ijk}^-\rangle_{abc} \right). \quad (12)$$

Here the subscripts  $i, j$ , and  $k \in \{0,1\}$ , and the polarization-encoded GHZ states  $|\text{GHZ}_{ijk}^\pm\rangle_{abc}$  are defined in Eq. (5) for  $n = 3$ . The eight distant stationary GHZ entanglements among Alice, Bob, and Charlie are of the following forms

$$\begin{aligned} |\text{GHZ}_{000}^\pm\rangle_{ABC} &= \frac{1}{\sqrt{2}} (|\uparrow\rangle_A |\uparrow\rangle_B |\uparrow\rangle_C \pm |\downarrow\rangle_A |\downarrow\rangle_B |\downarrow\rangle_C), \\ |\text{GHZ}_{100}^\pm\rangle_{ABC} &= \frac{1}{\sqrt{2}} (|\downarrow\rangle_A |\uparrow\rangle_B |\uparrow\rangle_C \pm |\uparrow\rangle_A |\downarrow\rangle_B |\downarrow\rangle_C), \\ |\text{GHZ}_{010}^\pm\rangle_{ABC} &= \frac{1}{\sqrt{2}} (|\uparrow\rangle_A |\downarrow\rangle_B |\uparrow\rangle_C \pm |\downarrow\rangle_A |\uparrow\rangle_B |\downarrow\rangle_C), \\ |\text{GHZ}_{001}^\pm\rangle_{ABC} &= \frac{1}{\sqrt{2}} (|\uparrow\rangle_A |\uparrow\rangle_B |\downarrow\rangle_C \pm |\downarrow\rangle_A |\downarrow\rangle_B |\uparrow\rangle_C), \end{aligned} \quad (13)$$

which constitute a complete basis for three-QD systems. When the ancillary node Eve performs a quantum swapping operation with a three-photon polarization-encoded GHZ-state analysis, the states of the three stationary qubits, which belong to Alice, Bob, and Charlie, are projected into a deterministic GHZ state according to the analysis result of Eve. That is, we can, in principle, generate multipartite GHZ entanglement efficiently among distant stationary qubits with a perfect efficiency.

In Sec. III, we have described a particular pattern of the GHZ-state analysis with a preset time delay between each two optical elements. Now we demonstrate that the GHZ-state analysis also works for a time-delay free pattern, by performing the aforementioned quantum swapping as an example. Suppose both QDs in the QND detectors are initialized in the state  $|+\rangle = (|\uparrow\rangle + |\downarrow\rangle)/\sqrt{2}$ , and all the linear-optical elements perform the same operation as that described in Sec. III. The three photons from hybrid entanglement pairs  $Aa$ ,  $Bb$ , and  $Cc$ , subsequently pass through the analysis setup independently, rather than transmitting them in a block pattern. After photon  $a$  passing through the setup and being routed into two spatial modes, which are ended with single-photon detectors, the hybrid system, consisting of three entanglement photon pairs and two QDs in the QND detectors, evolves into

$$\begin{aligned} |\Phi\rangle_1 &= \frac{1}{2} \left[ |H\rangle_a (|+\rangle_A |-\rangle_1 |+\rangle_2 + |-\rangle_A |+\rangle_1 |-\rangle_2) \right. \\ &\quad \left. - |V\rangle_a (|+\rangle_A |-\rangle_1 |+\rangle_2 - |-\rangle_A |+\rangle_1 |-\rangle_2) \right] \\ &\quad \otimes |\phi\rangle_{Bb} |\phi\rangle_{Cc}. \end{aligned} \quad (14)$$

For clarity, we assume that the standard (destructive) single-photon detectors work nondestructively and a photon survives after a measurement on it, such that we can directly specify the state of the distant stationary qubits

according to the state of the photon  $a$ . Subsequently, the photon  $b$  is input into the setup when the photon  $a$  has passed through the setup and lead to a click of either single-photon destructive detector. The hybrid system evolves into

$$\begin{aligned} |\Phi\rangle_2 &= \left[ (|\Phi^+\rangle_{AB} |+\rangle_1 |+\rangle_2 + |\Phi^-\rangle_{AB} |-\rangle_1 |-\rangle_2) |H\rangle_a |H\rangle_b \right. \\ &\quad - (|\Psi^+\rangle_{AB} |+\rangle_1 |+\rangle_2 + |\Psi^-\rangle_{AB} |-\rangle_1 |-\rangle_2) |H\rangle_a |V\rangle_b \\ &\quad - (|\Psi^+\rangle_{AB} |+\rangle_1 |+\rangle_2 - |\Psi^-\rangle_{AB} |-\rangle_1 |-\rangle_2) |V\rangle_a |H\rangle_b \\ &\quad \left. + (|\Phi^+\rangle_{AB} |+\rangle_1 |+\rangle_2 - |\Phi^-\rangle_{AB} |-\rangle_1 |-\rangle_2) |V\rangle_a |V\rangle_b \right] \\ &\quad \otimes |\phi\rangle_{Cc}, \end{aligned} \quad (15)$$

where the four Bell states of the two QDs, belonging to Alice and Bob, are as follows:

$$\begin{aligned} |\Phi^\pm\rangle_{AB} &= \frac{1}{\sqrt{2}} (|\uparrow\rangle_A |\uparrow\rangle_B \pm |\downarrow\rangle_A |\downarrow\rangle_B), \\ |\Psi^\pm\rangle_{AB} &= \frac{1}{\sqrt{2}} (|\uparrow\rangle_A |\downarrow\rangle_B \pm |\downarrow\rangle_A |\uparrow\rangle_B), \end{aligned} \quad (16)$$

Now, if Eve terminates the input of photon  $c$  and detects the two QDs of the QND detectors, the two distant QDs  $A$  and  $B$  are collapsed to one of the Bell states given in Eq. (16), according to the results of the QND detectors and the measurement on photons  $ab$ . That is, a deterministic quantum swapping operation can be completed between two hybrid entanglement pairs  $Aa$  and  $Bb$  by using the passive GHZ analysis setup.

If Eve inputs the photon  $c$  into the analysis setup rather than terminating it with a measurement on the two QDs of the QND detectors, the state  $|\Phi\rangle_2$  of the hybrid system evolves into the final state

$$\begin{aligned} |\Phi\rangle_3 &= \left[ |\text{GHZ}_{000}^+\rangle_{ABC} |\text{GHZ}_{000}^-\rangle_{abc} \right. \\ &\quad \left. - \sum_{ijk} |\text{GHZ}_{ijk}^+\rangle_{ABC} |\text{GHZ}_{ijk}^-\rangle_{abc} \right] |-\rangle_1 |+\rangle_2 \\ &\quad + \left[ |\text{GHZ}_{000}^-\rangle_{ABC} |\text{GHZ}_{000}^+\rangle_{abc} \right. \\ &\quad \left. - \sum_{ijk} |\text{GHZ}_{ijk}^+\rangle_{ABC} |\text{GHZ}_{ijk}^-\rangle_{abc} \right] |+\rangle_1 |-\rangle_2, \end{aligned} \quad (17)$$

where the subscripts  $i, j, k \in \{0,1\}$  and  $i+j+k = 1$ . This final state is identical to that obtained from Eq. (12) when a polarization-encoded GHZ-state analysis is applied on three photons of the hybrid entangled pairs, since three distant QDs  $A$ ,  $B$ , and  $C$  are projected into a predetermined GHZ state, according to the results of the QND detectors and the single-photon destructive detectors. Therefore, in principle, the passive GHZ-state analysis works faithfully for both cases, i.e., the time-delay and time-delay-free cases, when an ideal single-photon QND detector is available.

## V. PERFORMANCE OF THE PASSIVE GHZ-STATE ANALYSER

A core element of the passive GHZ-state analysis is the QND detector for single photons. Here a unit consisting of a QD and a micropillar cavity enables such a QND detection. In principle, the QND detector can perfectly distinguish two orthogonal polarization states  $|H\rangle$  and  $|V\rangle$  of a single photon with perfect efficiency. However, there are always some imperfections that introduce a deviation from ideal single-photon scattering [77–81], such as a finite single-photon bandwidth, a finite coupling  $g$  between a QD and a cavity, and the nondirectional cavity side leakage  $\kappa_s$ , etc. This leads to realistic (nonideal) scattering for a linearly-polarized photon. Thus, the hybrid system consisting of a linearly-polarized single photon and a QD, evolves as follows:

$$\begin{aligned} |H\rangle|\pm\rangle &\rightarrow \frac{1}{2}[(r_1 + r_0)|H\rangle|\pm\rangle + (r_1 - r_0)|V\rangle|\mp\rangle], \\ |V\rangle|\pm\rangle &\rightarrow \frac{1}{2}[(r_1 - r_0)|H\rangle|\mp\rangle + (r_1 + r_0)|V\rangle|\pm\rangle], \end{aligned} \quad (18)$$

where the parameters  $r$  and  $r_0$  are the reflection coefficients given in Eq. (2). After scattering, the state of the photon and the QD evolves in two ways independent of its initial state:

(1) It is flipped simultaneously with a probability  $p_1 = |r_1 - r_0|^2/4$ , which is the desired output and it can be simplified to perform an ideal QND detection, as given in Eq. (3), when ideal scattering with  $r_1 = 1$  and  $r = -1$  is achieved.

(2) The state of the photon and the QD are unchanged with the probability  $p_2 = |r_1 + r_0|^2/4$ , which leads to errors and results in an unfaithful QND detection for single photons.

Fortunately, this nonideal scattering does not affect the fidelity of the passive GHZ-state analysis, since the undesired scattering component is filtered out automatically by the PBS and only leads to an inconclusive result rather than infidelity result by a click of the single-photon destructive detector  $D_3$ .

Nonideal scattering in a practical QND detection does not reduce the fidelity of an  $n$ -photon GHZ analysis. However, this realistic scattering decreases the success efficiency  $\eta_n^s$ , which is defined as the probability that all photons are detected by a single-photon destructive detector, either  $D_1$  or  $D_2$ . For monochromatic photons of a frequency  $\omega$ , the efficiency  $\eta_n^s$  is defined as

$$\eta_n^s = \eta_0^n \eta_1^n(\omega), \quad (19)$$

where  $\eta_0$  is the efficiency of a single-photon detector  $D_i$  and  $\eta_1(\omega)$  is the error-free efficiency of a practical scattering with

$$\eta_1(\omega) = \frac{|r(\omega) - r_0(\omega)|^2}{4}. \quad (20)$$

The average efficiencies of the passive two-photon Bell-state and the three-photon GHZ-state analyzers are

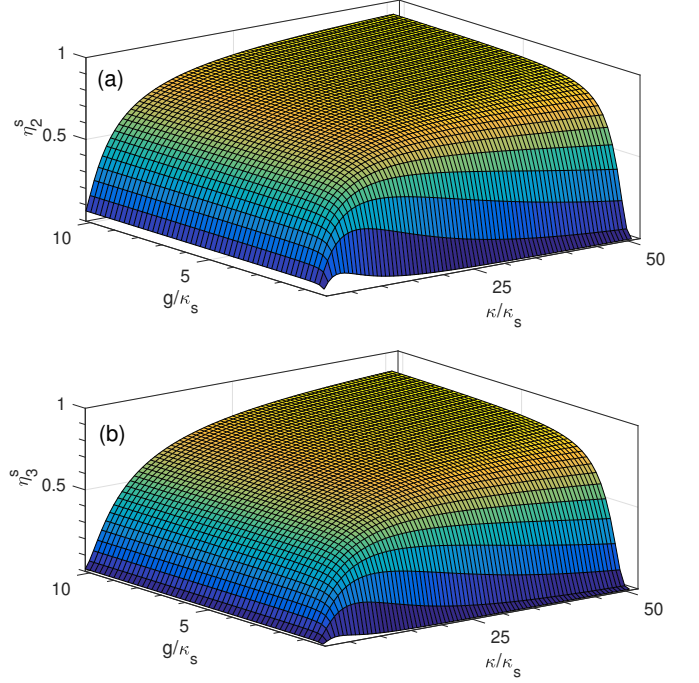


FIG. 4: Average efficiencies (a)  $\eta_2^s$  of the two-photon Bell-state analyzer and (b)  $\eta_3^s$  of the three-photon GHZ-state analyzer versus the coupling strength  $g/\kappa_s$  and the directional coupling rate of a cavity  $\kappa/\kappa_s$  in units of cavity side leakage  $\kappa_s$ . These averages are calculated over all detunings of input photons, with the Gaussian spectrum given by Eq. (21) and  $\sigma_\omega = \gamma$ . The decay parameters  $(\kappa_s, \gamma) = (30 \mu\text{eV}, 0.3 \mu\text{eV})$ .

shown in Fig. 4 with decay parameters  $(\kappa_s, \gamma) = (30 \mu\text{eV}, 0.3 \mu\text{eV})$ , which are adopted according to the QDs that are embedded in electrically controlled cavities around 4 K [88, 89]. We plotted the average efficiencies  $\eta_2^s$  and  $\eta_3^s$  versus the coupling strength  $g/\kappa_s$  and the directional coupling rate of the cavity  $\kappa/\kappa_s$  for a given Gaussian single-photon pulse defined by the spectrum

$$f(\omega) = \frac{1}{\sqrt{\pi}\sigma_\omega} \exp \left[ - \left( \frac{\omega - \omega_c}{\sigma_\omega} \right)^2 \right], \quad (21)$$

where  $\omega_c$  is the center frequency and  $\sigma_\omega$  denotes the pulse bandwidth with  $\omega_c = \omega_{X-}$  and  $\sigma_\omega = \gamma$ .

In general, the average efficiencies of the passive two-photon Bell-state and three-photon GHZ-state analyzers increase when the coupling  $g/\kappa_s$  between a QD and a cavity is increased for a given directional coupling rate  $\kappa/\kappa_s$ . This is because the cooperativity  $C = g^2/\gamma\kappa_T$  with  $\kappa_T = \kappa + \kappa_s$ , which is defined as an essential parameter quantifying the loss of an atom-cavity system, increases when we increase  $g/\kappa_s$  and keep other parameters unchanged. For a given  $g/\kappa_s$ , the average efficiencies of these two analyzers first increase and then decrease when  $\kappa/\kappa_s$  is increased, as shown in Fig. 4, although the cooperativity  $C$  decreases with an increased  $\kappa_T$ . Therefore, one can maximize the efficiencies by using cavities

of a mediate  $\kappa$ , which can be achieved, e.g., by decreasing the number of the Bragg reflector of a micropillar cavity. For simplicity, we set the efficiency of a single-photon destructive detector as  $\eta_0 = 1$ . For the two-photon Bell-state analyzer, its average efficiency  $\eta_2^s = 0.304$  for an experimental demonstrated coupling  $g/\kappa_s = 1$  and the directional coupling rate of a cavity,  $\kappa/\kappa_s = 3$ , which corresponds to a cooperativity  $C = 25$ . For the three-photon GHZ-state analyzer, one can obtain the average efficiency  $\eta_3^s \simeq 0.168$  for the same systematic parameters. If  $\kappa$  is increased to  $\kappa/\kappa_s = 19$  with a cooperativity  $C = 5$  [88], the average efficiencies of the passive two-photon Bell-state and three-photon GHZ-state analyzers are increased to  $\eta_2^s \simeq 0.664$  and  $\eta_3^s \simeq 0.541$ , respectively. This clearly shows that the passive analyzers are within reach of existing experimental capabilities. It is seen that their efficiencies are significantly higher than those consisting of linear-optical elements and single-photon detectors.

## VI. DISCUSSION AND SUMMARY

The GHZ-state analyzer based on linear optics can passively distinguish two GHZ states  $|\text{GHZ}_{00\dots 0}^\pm\rangle = (|H\rangle^{\otimes n} \pm |V\rangle^{\otimes n})/\sqrt{2}$  from the remaining  $(2^n - 2)$  GHZ states which, in principle, enables a complete analysis for  $2^n$  GHZ states when many ancillary photons and detectors are used [65]. This kind of GHZ analysis is much like a GHZ-state generation that is constructed by linear optics and post-selection [27, 53, 54]. Currently, the largest GHZ state of a ten-photon system has been demonstrated by using linear optics [90]. The existing GHZ-state analyzers, which are based on optical nonlinearities, have been proposed by cascading two-photon parity QND detectors [20, 91]. Such an analyzer can, in principle, distinguish  $2^n$  GHZ states of  $n$ -photon system nondestructively, when it is assisted by fast switching and/or active operations during the entangled-state analysis. These operations dramatically increase its experimental complexity and consume more quantum resources. Furthermore, such implementations always require a strong optical nonlinearity to keep the entangled-state analysis faithful.

Our scheme of a passive GHZ-state analysis for  $n$  polarization-encoded photons uses only linear-optical elements, and single-photon destructive and nondestructive detectors. This analyzer can, in principle, deterministically distinguish among  $2^n$  GHZ states for  $n$ -photon systems, and hence it combines the advantages of those based on linear optics with those based on optical nonlinearities. Moreover, our scheme eliminates disadvantages of such standard analyzers by designing an error-tolerance QND detection for single photons.

The proposed QND detector consists of a four-level emitter coupled to a microcavity or waveguide [76–81], such as a negatively charged QD coupled to a micropillar cavity. This analyzer is compatible with existing QND

proposals [80, 83, 84] for single photons; however, as we have shown, it is more efficient than the standard ones for several reasons: Our QND detector can work in a passive way and can faithfully distinguish photon numbers subsequently passing through it in an even/odd basis. Furthermore, it is error-tolerant, when it is used to detect linearly-polarized photons.

Our description of scattering imperfections included: finite photon-pulse bandwidth  $\sigma_\omega$ , cavity loss  $\kappa_s$ , and finite coupling  $g$ . This realistic scattering process leads to a hybrid entangled state of a photon and a QD, consisting of ideal scattering component and the error scattering component. The error component is passively filtered out by a PBS and then is heralded by a click of a single-photon destructive detector, leading to an inconclusive result rather than an unfaithful GHZ-state analysis.

Furthermore, the QD is one of the most promising candidates for quantum information processing due to its very good characteristics concerning optical initialization, single-qubit manipulation and readout, and the well-developed semiconductor technology [87, 92–94]. Recently, a five-photon polarization-encoded cluster state has been demonstrated with a confined dark exciton in a QD [95] and an all-photonic quantum repeater protocol was presented with a similar solid-state four-level emitter [96].

In summary, we have proposed a passive GHZ-state analyzer for polarization-encoded photons based on linear optics and single-photon QND detectors. An error-tolerant QND detector for polarization-encoded photons, consisting of a QD and a microcavity, is proposed to distinguish the number of photons passing through it in the basis with either even or odd photon numbers. This QND detector constitutes a faithful element for the GHZ-state analyzer setup by introducing a passively error-filtering structure with linear optics. There are neither active operations nor adaptive switching in the proposed method, since the faithful GHZ-state analysis for multiple photon systems works efficiently by passively arranging two QND detectors, single-photon destructive detectors, and linear-optical elements. Furthermore, the described method is universal, as it enables two-photon Bell-state and multiphoton GHZ-state analyses. All these distinct characteristics make the proposed passive analyzers simple and resource-efficient for long-distance multimode quantum communication and quantum networks.

## Acknowledgments

T.L. and K.X. acknowledge the support of the National Key R&D Program of China (Grant No. 2017YFA0303703) and the Natural Science Foundation of Jiangsu Province (Grant No. BK20180461). A.M. and F.N. acknowledge a grant from the John Templeton Foundation. F.N. is also supported in part by the:



MURI Center for Dynamic Magneto-Optics via the Air Force Office of Scientific Research (AFOSR) (FA9550-14-1-0040), Army Research Office (ARO) (Grant No. Grant No. W911NF-18-1-0358), Asian Office of Aerospace Research and Development (AOARD) (Grant No. FA2386-18-1-4045), Japan Science and Technology Agency (JST) (Q-LEAP program, ImPACT program, and CREST Grant No. JPMJCR1676), , Japan Society for the Promotion of Science (JSPS) (JSPS-RFBR Grant No. 17-52-

50023, and JSPS-FWO Grant No. VS.059.18N), RIKEN-AIST Challenge Research Fund, and the John Templeton Foundation.

## References

- 
- [1] R. Horodecki, P. Horodecki, M. Horodecki, and K. Horodecki, “Quantum entanglement,” *Rev. Mod. Phys.* **81**, 865 (2009).
  - [2] H. J. Kimble, “The quantum internet,” *Nature* **453**, 1023–1030 (2008).
  - [3] J. I. Cirac, A. K. Ekert, S. F. Huelga, and C. Macchiavello, “Distributed quantum computation over noisy channels,” *Phys. Rev. A* **59**, 4249–4254 (1999).
  - [4] Y. L. Lim, A. Beige, and L. C. Kwek, “Repeat-until-success linear optics distributed quantum computing,” *Phys. Rev. Lett.* **95**, 030505 (2005).
  - [5] L. Jiang, J. M. Taylor, A. S. Sørensen, and M. D. Lukin, “Distributed quantum computation based on small quantum registers,” *Phys. Rev. A* **76**, 062323 (2007).
  - [6] W. Qin, X. Wang, A. Miranowicz, Z. Zhong, and F. Nori, “Heralded quantum controlled-phase gates with dissipative dynamics in macroscopically distant resonators,” *Phys. Rev. A* **96**, 012315 (2017).
  - [7] H.-K. Lo, M. Curty, and K. Tamaki, “Secure quantum key distribution,” *Nat. Photon.* **8**, 595 (2014).
  - [8] S. Pirandola, J. Eisert, C. Weedbrook, A. Furusawa, and S. L. Braunstein, “Advances in quantum teleportation,” *Nat. photon.* **9**, 641 (2015).
  - [9] G.-L. Long and X.-S. Liu, “Theoretically efficient high-capacity quantum-key-distribution scheme,” *Phys. Rev. A* **65**, 032302 (2002).
  - [10] F.-G. Deng, G. L. Long, and X.-S. Liu, “Two-step quantum direct communication protocol using the Einstein-Podolsky-Rosen pair block,” *Phys. Rev. A* **68**, 042317 (2003).
  - [11] J.-Y. Hu, B. Yu, M.-Y. Jing, L.-T. Xiao, S.-T. Jia, G.-Q. Qin, and G.-L. Long, “Experimental quantum secure direct communication with single photons,” *Light Sci. Appl.* **5**, e16144 (2016).
  - [12] W. Zhang, D.-S. Ding, Y.-B. Sheng, L. Zhou, B.-S. Shi, and G.-C. Guo, “Quantum secure direct communication with quantum memory,” *Phys. Rev. Lett.* **118**, 220501 (2017).
  - [13] N. Gisin, G. Ribordy, W. Tittel, and H. Zbinden, “Quantum cryptography,” *Rev. Mod. Phys.* **74**, 145–195 (2002).
  - [14] W. Dür, H.-J. Briegel, J. Cirac, and P. Zoller, “Quantum repeaters based on entanglement purification,” *Phys. Rev. A* **59**, 169 (1999).
  - [15] L. Jiang, J. M. Taylor, K. Nemoto, W. J. Munro, R. Van Meter, and M. D. Lukin, “Quantum repeater with encoding,” *Phys. Rev. A* **79**, 032325 (2009).
  - [16] T.-J. Wang, S.-Y. Song, and G. L. Long, “Quantum repeater based on spatial entanglement of photons and quantum-dot spins in optical microcavities,” *Phys. Rev. A* **85**, 062311 (2012).
  - [17] W. J. Munro, A. M. Stephens, S. J. Devitt, K. A. Harrison, and K. Nemoto, “Quantum communication without the necessity of quantum memories,” *Nat. Photon.* **6**, 777–781 (2012).
  - [18] C. H. Bennett, G. Brassard, S. Popescu, B. Schumacher, J. A. Smolin, and W. K. Wootters, “Purification of noisy entanglement and faithful teleportation via noisy channels,” *Phys. Rev. Lett.* **76**, 722–725 (1996).
  - [19] D. Deutsch, A. Ekert, R. Jozsa, C. Macchiavello, S. Popescu, and A. Sanpera, “Quantum privacy amplification and the security of quantum cryptography over noisy channels,” *Phys. Rev. Lett.* **77**, 2818–2821 (1996).
  - [20] Y.-B. Sheng, F.-G. Deng, and H.-Y. Zhou, “Efficient polarization-entanglement purification based on parametric down-conversion sources with cross-Kerr nonlinearity,” *Phys. Rev. A* **77**, 042308 (2008).
  - [21] Y.-B. Sheng and F.-G. Deng, “Deterministic entanglement purification and complete nonlocal Bell-state analysis with hyperentanglement,” *Phys. Rev. A* **81**, 032307 (2010).
  - [22] M. Żukowski, A. Zeilinger, M. A. Horne, and A. K. Ekert, ““Event-ready-detectors” Bell experiment via entanglement swapping,” *Phys. Rev. Lett.* **71**, 4287–4290 (1993).
  - [23] L. Chen and W. She, “Hybrid entanglement swapping of photons: Creating the orbital angular momentum Bell states and Greenberger-Horne-Zeilinger states,” *Phys. Rev. A* **83**, 012306 (2011).
  - [24] C. Y. Hu and J. G. Rarity, “Loss-resistant state teleportation and entanglement swapping using a quantum-dot spin in an optical microcavity,” *Phys. Rev. B* **83**, 115303 (2011).
  - [25] Y.-N. Chen, S.-L. Chen, N. Lambert, C.-M. Li, G.-Y. Chen, and F. Nori, “Entanglement swapping and testing quantum steering into the past via collective decay,” *Phys. Rev. A* **88**, 052320 (2013).
  - [26] X. Su, C. Tian, X. Deng, Q. Li, C. Xie, and K. Peng, “Quantum entanglement swapping between two multipartite entangled states,” *Phys. Rev. Lett.* **117**, 240503 (2016).
  - [27] J.-W. Pan, Z.-B. Chen, C.-Y. Lu, H. Weinfurter, A. Zeilinger, and M. Żukowski, “Multiphoton entanglement and interferometry,” *Rev. Mod. Phys.* **84**, 777 (2012).
  - [28] F.-G. Deng, B.-C. Ren, and X.-H. Li, “Quantum hyperentanglement and its applications in quantum information processing,” *Sci. Bull.* **62**, 46 – 68 (2017).
  - [29] T. Tashima, M. S. Tame, S. K. Özdemir, F. Nori,

- M. Koashi, and H. Weinfurter, “Photonic multipartite entanglement conversion using nonlocal operations,” *Phys. Rev. A* **94**, 052309 (2016).
- [30] M. Hillery, V. Bužek, and A. Berthiaume, “Quantum secret sharing,” *Phys. Rev. A* **59**, 1829–1834 (1999).
- [31] S. Schauer, M. Huber, and B. C. Hiesmayr, “Experimentally feasible security check for  $n$ -qubit quantum secret sharing,” *Phys. Rev. A* **82**, 062311 (2010).
- [32] A. Farouk, J. Batle, M. Elhoseny, M. Naseri, M. Lone, A. Fedorov, M. Alkhambashi, S. H. Ahmed, and M. Abdel-Aty, “Robust general  $N$  user authentication scheme in a centralized quantum communication network via generalized GHZ states,” *Front. Phys.* **13**, 130306 (2018).
- [33] L. Dong, Y.-F. Lin, C. Cui, H.-K. Dong, X.-M. Xiu, and Y.-J. Gao, “Fault-tolerant distribution of GHZ states and controlled DSQC based on parity analyses,” *Opt. Express* **25**, 18581–18591 (2017).
- [34] H. J. Briegel, D. E. Browne, W. Dür, R. Raussendorf, and M. Van den Nest, “Measurement-based quantum computation,” *Nat. Phys.* **5**, 19 (2009).
- [35] T. Tanamoto, Y.-X. Liu, S. Fujita, X. Hu, and F. Nori, “Producing cluster states in charge qubits and flux qubits,” *Phys. Rev. Lett.* **97**, 230501 (2006).
- [36] J. Q. You, X.-B. Wang, T. Tanamoto, and F. Nori, “Efficient one-step generation of large cluster states with solid-state circuits,” *Phys. Rev. A* **75**, 052319 (2007).
- [37] T. Tanamoto, Y.-X. Liu, X. Hu, and F. Nori, “Efficient quantum circuits for one-way quantum computing,” *Phys. Rev. Lett.* **102**, 100501 (2009).
- [38] S. E. Economou, N. Lindner, and T. Rudolph, “Optically generated 2-dimensional photonic cluster state from coupled quantum dots,” *Phys. Rev. Lett.* **105**, 093601 (2010).
- [39] M. Gimeno-Segovia, P. Shadbolt, D. E. Browne, and T. Rudolph, “From three-photon Greenberger-Horne-Zeilinger states to ballistic universal quantum computation,” *Phys. Rev. Lett.* **115**, 020502 (2015).
- [40] Y. Li, P. C. Humphreys, G. J. Mendoza, and S. C. Benjamin, “Resource costs for fault-tolerant linear optical quantum computing,” *Phys. Rev. X* **5**, 041007 (2015).
- [41] L. F. Wei, Y.-x. Liu, and F. Nori, “Generation and control of Greenberger-Horne-Zeilinger entanglement in superconducting circuits,” *Phys. Rev. Lett.* **96**, 246803 (2006).
- [42] Y.-D. Wang, S. Chesi, D. Loss, and C. Bruder, “One-step multiqubit Greenberger-Horne-Zeilinger state generation in a circuit QED system,” *Phys. Rev. B* **81**, 104524 (2010).
- [43] T. Monz, P. Schindler, J. T. Barreiro, M. Chwalla, D. Nigg, W. A. Coish, M. Harlander, W. Hänsel, M. Hennrich, and R. Blatt, “14-qubit entanglement: Creation and coherence,” *Phys. Rev. Lett.* **106**, 130506 (2011).
- [44] H. Kaufmann, T. Ruster, C. T. Schmiegelow, M. A. Luda, V. Kaushal, J. Schulz, D. von Lindenfels, F. Schmidt-Kaler, and U. G. Poschinger, “Scalable creation of long-lived multipartite entanglement,” *Phys. Rev. Lett.* **119**, 150503 (2017).
- [45] C.-S. Yu, X. X. Yi, H.-S. Song, and D. Mei, “Robust preparation of Greenberger-Horne-Zeilinger and  $W$  states of three distant atoms,” *Phys. Rev. A* **75**, 044301 (2007).
- [46] A. Zheng, J. Li, R. Yu, X.-Y. Lü, and Y. Wu, “Generation of Greenberger-Horne-Zeilinger state of distant diamond nitrogen-vacancy centers via nanocavity input-output process,” *Opt. Express* **20**, 16902–16912 (2012).
- [47] F. Reiter, D. Reeb, and A. S. Sørensen, “Scalable dissipative preparation of many-body entanglement,” *Phys. Rev. Lett.* **117**, 040501 (2016).
- [48] X. Q. Shao, J. H. Wu, X. X. Yi, and G.-L. Long, “Dissipative preparation of steady Greenberger-Horne-Zeilinger states for Rydberg atoms with quantum Zeno dynamics,” *Phys. Rev. A* **96**, 062315 (2017).
- [49] Y.-F. Huang, B.-H. Liu, L. Peng, Y.-H. Li, L. Li, C.-F. Li, and G.-C. Guo, “Experimental generation of an eight-photon Greenberger-Horne-Zeilinger state,” *Nat. Commun.* **2**, 546 (2011).
- [50] X.-C. Yao, T.-X. Wang, P. Xu, H. Lu, G.-S. Pan, X.-H. Bao, C.-Z. Peng, C.-Y. Lu, Y.-A. Chen, and J.-W. Pan, “Observation of eight-photon entanglement,” *Nat. Photon.* **6**, 225–228 (2012).
- [51] M. Malik, M. Erhard, M. Huber, M. Krenn, R. Fickler, and A. Zeilinger, “Multi-photon entanglement in high dimensions,” *Nat. Photon.* **10**, 248 (2016).
- [52] M. Krenn, M. Malik, R. Fickler, R. Lapkiewicz, and A. Zeilinger, “Automated search for new quantum experiments,” *Phys. Rev. Lett.* **116**, 090405 (2016).
- [53] M. Krenn, A. Hochrainer, M. Lahiri, and A. Zeilinger, “Entanglement by path identity,” *Phys. Rev. Lett.* **118**, 080404 (2017).
- [54] N. Bergamasco, M. Menotti, J. E. Sipe, and M. Liscidini, “Generation of path-encoded Greenberger-Horne-Zeilinger states,” *Phys. Rev. Applied* **8**, 054014 (2017).
- [55] E. Megidish, T. Shacham, A. Halevy, L. Dovrat, and H. S. Eisenberg, “Resource efficient source of multiphoton polarization entanglement,” *Phys. Rev. Lett.* **109**, 080504 (2012).
- [56] L.-M. Duan and H. Kimble, “Scalable photonic quantum computation through cavity-assisted interactions,” *Phys. Rev. Lett.* **92**, 127902 (2004).
- [57] Y. Li, L. Aolita, and L. C. Kwak, “Photonic multiqubit states from a single atom,” *Phys. Rev. A* **83**, 032313 (2011).
- [58] Y. Hao, G. Lin, K. Xia, X. Lin, Y. Niu, and S. Gong, “Quantum controlled-phase-flip gate between a flying optical photon and a Rydberg atomic ensemble,” *Sci. Rep.* **5**, 10005 (2015).
- [59] A. Reiserer, N. Kalb, G. Rempe, and S. Ritter, “A quantum gate between a flying optical photon and a single trapped atom,” *Nature* **508**, 237–240 (2014).
- [60] A. Reiserer and G. Rempe, “Cavity-based quantum networks with single atoms and optical photons,” *Rev. Mod. Phys.* **87**, 1379 (2015).
- [61] S. Perseguers, G. Lapeyre Jr, D. Cavalcanti, M. Lewenstein, and A. Acín, “Distribution of entanglement in large-scale quantum networks,” *Rep. Prog. Phys.* **76**, 096001 (2013).
- [62] S. Bose, V. Vedral, and P. L. Knight, “Multiparticle generalization of entanglement swapping,” *Phys. Rev. A* **57**, 822 (1998).
- [63] C.-Y. Lu, T. Yang, and J.-W. Pan, “Experimental multiparticle entanglement swapping for quantum networking,” *Phys. Rev. Lett.* **103**, 020501 (2009).
- [64] J.-W. Pan and A. Zeilinger, “Greenberger-Horne-Zeilinger-state analyzer,” *Phys. Rev. A* **57**, 2208–2211 (1998).
- [65] P. Kok, W. J. Munro, K. Nemoto, T. C. Ralph, J. P. Dowling, and G. J. Milburn, “Linear optical quantum

- computing with photonic qubits,” *Rev. Mod. Phys.* **79**, 135–174 (2007).
- [66] J. Calsamiglia and N. Lütkenhaus, “Maximum efficiency of a linear-optical Bell-state analyzer,” *Appl. Phys. B* **72**, 67–71 (2001).
- [67] J. Qian, X.-L. Feng, and S.-Q. Gong, “Universal Greenberger-Horne-Zeilinger-state analyzer based on two-photon polarization parity detection,” *Phys. Rev. A* **72**, 052308 (2005).
- [68] Y. Xia, Y.-H. Kang, and P.-M. Lu, “Complete polarized photons Bell-states and Greenberger-Horne-Zeilinger-states analysis assisted by atoms,” *J. Opt. Soc. Am. B* **31**, 2077–2082 (2014).
- [69] L. Zhou and Y.-B. Sheng, “Complete logic Bell-state analysis assisted with photonic Faraday rotation,” *Phys. Rev. A* **92**, 042314 (2015).
- [70] Y.-B. Sheng, F.-G. Deng, and G. L. Long, “Complete hyperentangled-Bell-state analysis for quantum communication,” *Phys. Rev. A* **82**, 032318 (2010).
- [71] B.-C. Ren, H.-R. Wei, M. Hua, T. Li, and F.-G. Deng, “Complete hyperentangled-Bell-state analysis for photon systems assisted by quantum-dot spins in optical microcavities,” *Opt. Express* **20**, 24664–24677 (2012).
- [72] T.-J. Wang, Y. Lu, and G. L. Long, “Generation and complete analysis of the hyperentangled Bell state for photons assisted by quantum-dot spins in optical microcavities,” *Phys. Rev. A* **86**, 042337 (2012).
- [73] Q. Liu and M. Zhang, “Generation and complete non-destructive analysis of hyperentanglement assisted by nitrogen-vacancy centers in resonators,” *Phys. Rev. A* **91**, 062321 (2015).
- [74] G.-Y. Wang, Q. Ai, B.-C. Ren, T. Li, and F.-G. Deng, “Error-detected generation and complete analysis of hyperentangled Bell states for photons assisted by quantum-dot spins in double-sided optical microcavities,” *Opt. Express* **24**, 28444–28458 (2016).
- [75] D. Witthaut, M. D. Lukin, and A. S. Sørensen, “Photon sorters and QND detectors using single photon emitters,” *Europhys. Lett.* **97**, 50007 (2012).
- [76] J. P. Reithmaier, G. Sek, A. Löffler, C. Hofmann, S. Kuhn, S. Reitzenstein, L. Keldysh, V. Kulakovskii, T. Reinecke, and A. Forchel, “Strong coupling in a single quantum dot-semiconductor microcavity system,” *Nature* **432**, 197 (2004).
- [77] M. Arcari, I. Söllner, A. Javadi, S. Lindskov Hansen, S. Mahmoodian, J. Liu, H. Thyrrestrup, E. H. Lee, J. D. Song, S. Stobbe, and P. Lodahl, “Near-unity coupling efficiency of a quantum emitter to a photonic crystal waveguide,” *Phys. Rev. Lett.* **113**, 093603 (2014).
- [78] T. Li, A. Miranowicz, X. Hu, K. Xia, and F. Nori, “Quantum memory and gates using a  $\Lambda$ -type quantum emitter coupled to a chiral waveguide,” *Phys. Rev. A* **97**, 062318 (2018).
- [79] P. Lodahl, S. Mahmoodian, and S. Stobbe, “Interfacing single photons and single quantum dots with photonic nanostructures,” *Rev. Mod. Phys.* **87**, 347 (2015).
- [80] C. Y. Hu, A. Young, J. L. O’Brien, W. J. Munro, and J. G. Rarity, “Giant optical Faraday rotation induced by a single-electron spin in a quantum dot: applications to entangling remote spins via a single photon,” *Phys. Rev. B* **78**, 085307 (2008).
- [81] C. Y. Hu, W. J. Munro, and J. G. Rarity, “Deterministic photon entangler using a charged quantum dot inside a microcavity,” *Phys. Rev. B* **78**, 125318 (2008).
- [82] R. J. Warburton, “Single spins in self-assembled quantum dots,” *Nature Mater.* **12**, 483 (2013).
- [83] D. Witthaut and A. S. Sørensen, “Photon scattering by a three-level emitter in a one-dimensional waveguide,” *New J. Phys.* **12**, 043052 (2010).
- [84] A. Reiserer, S. Ritter, and G. Rempe, “Nondestructive detection of an optical photon,” *Science* **342**, 1349–1351 (2013).
- [85] Y. Li, L. Aolita, D. E. Chang, and L. C. Kwek, “Robust-fidelity atom-photon entangling gates in the weak-coupling regime,” *Phys. Rev. Lett.* **109**, 160504 (2012).
- [86] T. Li and F.-G. Deng, “Error-rejecting quantum computing with solid-state spins assisted by low- $q$  optical microcavities,” *Phys. Rev. A* **94**, 062310 (2016).
- [87] I. Buluta, S. Ashhab, and F. Nori, “Natural and artificial atoms for quantum computation,” *Rep. Prog. Phys.* **74**, 104401 (2011).
- [88] V. Giesz, N. Somaschi, G. Hornecker, T. Grange, B. Reznichenko, L. De Santis, J. Demory, C. Gomez, I. Sagnes, A. Lemaître, *et al.*, “Coherent manipulation of a solid-state artificial atom with few photons,” *Nat. Commun.* **7**, 11986 (2016).
- [89] N. Somaschi, V. Giesz, L. De Santis, J. Loredó, M. P. Almeida, G. Hornecker, S. L. Portalupi, T. Grange, C. Antón, J. Demory, C. Gómez, I. Sagnes, N. D. Lanzillotti-Kimura, A. Lemaître, A. Auffeves, A. G. White, L. Lanco, and P. Senellart, “Near-optimal single-photon sources in the solid state,” *Nat. Photon.* **10**, 340 (2016).
- [90] L.-K. Chen, Z.-D. Li, X.-C. Yao, M. Huang, W. Li, H. Lu, X. Yuan, Y.-B. Zhang, X. Jiang, C.-Z. Peng, L. Li, N.-L. Liu, X. Ma, C.-Y. Lu, Y.-A. Chen, and J.-W. Pan, “Observation of ten-photon entanglement using thin  $\text{BiB}_3\text{O}_6$  crystals,” *Optica* **4**, 77–83 (2017).
- [91] T. B. Pittman, B. C. Jacobs, and J. D. Franson, “Demonstration of nondeterministic quantum logic operations using linear optical elements,” *Phys. Rev. Lett.* **88**, 257902 (2002).
- [92] R.-B. Liu, W. Yao, and L. Sham, “Quantum computing by optical control of electron spins,” *Adv. Phys.* **59**, 703–802 (2010).
- [93] K. De Greve, D. Press, P. L. McMahon, and Y. Yamamoto, “Ultrafast optical control of individual quantum dot spin qubits,” *Rep. Prog. Phys.* **76**, 092501 (2013).
- [94] P. Lodahl, “Quantum-dot based photonic quantum networks,” *Quantum Sci. Technol.* **3**, 013001 (2017).
- [95] I. Schwartz, D. Cogan, E. R. Schmidgall, Y. Don, L. Gantz, O. Kenneth, N. H. Lindner, and D. Gershoni, “Deterministic generation of a cluster state of entangled photons,” *Science* **354**, 434–437 (2016).
- [96] D. Buterakos, E. Barnes, and S. E. Economou, “Deterministic generation of all-photonic quantum repeaters from solid-state emitters,” *Phys. Rev. X* **7**, 041023 (2017).